



**Thermal Modelling of Hybrid Composites of nano  
cenosphere and Polycarbonate for Thermal Protection  
System**

Journal:	<i>RSC Advances</i>
Manuscript ID:	RA-ART-08-2014-007973.R1
Article Type:	Paper
Date Submitted by the Author:	28-Aug-2014
Complete List of Authors:	KATIYAR, NEHA; DIAT (DU), MATERIALS ENGINEERING KANDASUBRAMANIAN, BALASUBRAMANIAN; DIAT(DU), METARIALS ENGINEERING

Cite this: DOI: 10.1039/c0xx00000x

www.rsc.org/xxxxxx

PAPER

# Thermal Modelling of Hybrid Composites of nano cenosphere and Polycarbonate for Thermal Protection System

Neha Katiyar<sup>a</sup>, Balasubramanian K<sup>\*a</sup>*Received (in XXX, XXX) Xth XXXXXXXXXX 20XX, Accepted Xth XXXXXXXXXX 20XX*

DOI: 10.1039/b000000x

The disposal of Fly ash cenosphere is a heavy challenge for various coal and thermal power plants. In this perspective, the present research work aims at using the waste product of thermal power plants as filler in engineering plastic as an alternative to thermosets as matrices for high performance composites. The Fly ash cenosphere (FAC) fillers reinforced polycarbonate (PC) composites were fabricated using an economically and environmentally viable method of melt extrusion with varying concentration of filler as 5, 10, 20, 30, 40 and 50 wt%. FESEM were carried out/executed to examine the morphology of composite which reflects a good dispersion and strong interfacial interaction between PC and modified FAC than the unmodified counterpart. The characteristic peak appears at 2363 and 2930 cm<sup>-1</sup> in the FTIR corroborate the interaction between cenosphere particles and silane coupling agent. Thermogravimetric analysis (TGA) substantiate that PC-FAC had good thermal stability with high char yield 70% (which is almost thrice than that for unfilled PC) at 700°C in nitrogen atmosphere. The XRD pattern displays the characteristic peaks at (002) (100) and (110) which affirms the presence of turbostratic carbon that have crumbled hexagonal structure. Effective thermal conductivity of the composite was mathematically expressed by Maxwell model of thermal conductivity and the computed value was 0.13 W/m-°C with 29% decrement as compared to pristine PC.

## 1. INTRODUCTION

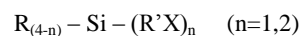
The dilating need of electric power in the world has led to tremendous production of electricity, 41% of which is obtained from coal fired power plants [1,2]. Coal-fired power plants, besides providing/contributing for a tremendous fraction of the global electricity, also produce an aluminosilicate rich mineral waste known as Fly Ash. The disposal of this waste is an emerging challenge and presently, slurry method is adopted in ash ponds [3]. This fly ash produced from pulverized combustion of coal, contains hollow aluminosilicate microspheres with a low bulk density of 0.2–0.8 g/cm<sup>3</sup>, namely, cenospheres. The content of cenospheres in fly ash varies over a rather wide range from 0.01 to 4.80 wt % and, in most cases, amounts to 0.3–1.5 wt % [4–7]. In general, the major component composition of cenosphere concentrates varies in the ranges of 50–65 wt % SiO<sub>2</sub>, 20–37 wt % Al<sub>2</sub>O<sub>3</sub>, and 1–11 wt % Fe<sub>2</sub>O<sub>3</sub> [4,6,8–13]. The Mullite content (3Al<sub>2</sub>O<sub>3</sub>·2SiO<sub>2</sub>) of cenospheres is responsible for their high/tremendous thermal stability, low thermal expansion, high

*Department of Materials Engineering, DIAT (DU), Girinagar, Pune, Maharashtra, Ministry of Defence, Email: [neha.katiyar1690@gmail.com](mailto:neha.katiyar1690@gmail.com)*

*\*Department of Materials Engineering, DIAT (DU), Girinagar, Pune, Maharashtra, Ministry of Defence, Email: [meetkbs@gmail.com](mailto:meetkbs@gmail.com), Fax: (020) 2438-9509, Tel (020) 2438-9680*

creep resistance in excessive oxidative and corrosive environments and high thermal shock resistance [14–19]. Cenospheres have been incorporated as fillers in various polymeric systems such as polyethylene, polypropylene, vinyl esters, polyamides [3, 20–22] owing to their low density, strong filling ability and excellent fluidity, which also play a vital role in reducing the cost of the composite. These systems involve surface treated cenospheres which enhance thermal properties. A plenty of work and literature has been reported, which cites the improvement in thermal properties of the composite containing cenosphere, but the composites of cenosphere with heat resistant thermoplastic polymers like polycarbonates for enhancement of flame retardancy are scantily known.

Polycarbonate (PC) is a kind of extensively applied engineering thermoplastic which exhibits distinguished mechanical properties, electrical insulation, thermal stability, extrudability and the ability to be processed on conventional machinery [23]. Despite its excellent physical properties, the restriction on its thermal properties limits its application and working life/workability. Polycarbonates (PC) are long chain linear polyesters of carbonic acids and dihydric phenols, which involve intermolecular attraction between the phenyl groups on the molecular chain. This contributes to molecular stiffness and lack of mobility of the individual molecules, which primarily explains the thermal stability of polycarbonates [24]. The present study represents a novel platform with a simple approach to enhance interfacial



Where R is alkoxy group

X is Organofunctionality

attraction and thermal resistance of hybrid organic – inorganic material, by direct melt reactive blending of PC with varying amount of silane treated FAC. This work proposes a method for reconciling the requirements for melt mixing by a facile route of synthesis of PC/FAC composite in our laboratory with varying weight % (5, 10, 20, 30, 40 and 50) of FAC. The paper exploits the potential application of surface treated Fly Ash cenospheres with polycarbonate for thermal insulative purpose, thus increasing the cost effectiveness of the composite. The composite of PC/FAC was melt blended in co-rotating twin screw extruder with 40:1 L/D ratio, the temperature of the screw was set to 280°C, speed of the screw was adjusted to 22 rpm and torque in the range of 40-50 N-m. Mathematical model for thermal conductivity of the composite was devised to reassert the insulative behavior of the cenosphere particles in the polymer matrix. FTIR and XRD studies were performed on the composite for compositional analysis while XRD confirms the presence of turbostratic carbon. Morphological attribution of grafted FAC was observed by FESEM. The thermal properties of the PC/FAC composite were analysed in terms of char residue by Thermogravimetric Analysis (TGA). The thermal decomposition behaviour was validated by mathematical modeling of thermal conductivity.

## 2. EXPERIMENTAL WORK

### 2.1 Materials

The PC used in this study was supplied by SABIC Innovative Plastics, India under the trade name LEXAN 143R, having Melt Flow Index (MFI) 10.5 g/10 min [ASTM D 1238]. Fly ash cenospheres, particle size ranging from 10nm to 90µm was obtained by CSRL-Structwel LAB Private Limited, Pune, India with chemical composition of 46.36 wt% SiO<sub>2</sub>, 42.08 wt% Al<sub>2</sub>O<sub>3</sub>, 2.12 wt% Fe<sub>2</sub>O<sub>3</sub>, 0.79 wt% MgO, 3.17 wt% SO<sub>3</sub>. The silane coupling agent, tetraethoxysilane was procured from SIGMA-ALDRICH and used as received.

### 2.2 Functionalization of Cenosphere

FAC's are inherently complete inorganic minerals, thus the molecular level adhesion between these fillers and organic polymers poses severe challenge. The surface of the FACs had to be chemically modified to achieve molecular miscibility and homogeneity. Silane Grafted Cenosphere was produced by grafting tetraethoxysilane onto cenosphere. The functionalization reaction of raw cenosphere was carried out by introducing 50 g FAC in an ethanol-water solution of 32:8 v/v and maintaining the temperature at 15°C. Silane coupling agent Tetraethoxysilane (3 wt% of cenosphere) was added to the solution and the resultant mixture was stirred for 1 hour at 40°C for uniform distribution and hydrolysis reaction. Bi-functionality of the silane molecules is must, so that they can react with two different phases and thereby forming a link between them. The alkoxy silanes have been demonstrated to be able to directly react with –Si-OH groups of silica and thereby forming –Si-O-Si bonds [25]. They have general chemical formula as:

Silane coupling agents reacted with water (hydrolysis) to form silanol groups and siloxane bonding via partial condensation. The silanol groups were attached to the surface of the inorganic material through hydrogen bonding. Finally, the inorganic material underwent a drying process and robust chemical bonds were formed through a dehydration condensation reaction [26] as Fig 1 shows the silane grafting of cenosphere. The mixture was subsequently dried in vacuum oven for 24 hours at 80°C. FTIR analysis was carried out to ensure the distribution of coupling agent on the surface of FAC and the formation of new characteristic peaks of silane coupling agent which affirmed the presence of silane agent on the surface of cenosphere particles.

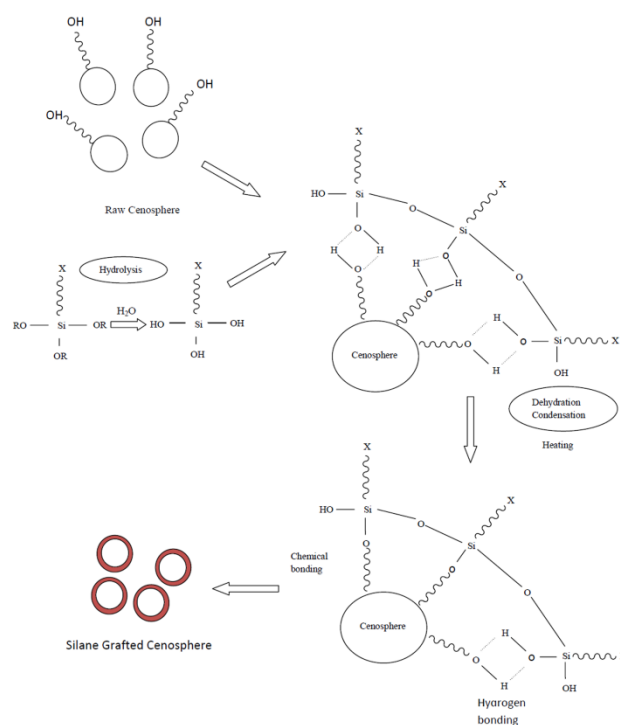


Fig.1 - Schematic representation of Silane Grafting of cenosphere [27]

### 2.3 Reactive Blending of Composite

The particulate composites of PC/cenosphere were prepared by melt extrusion of polycarbonate. The cenosphere particles used for the blending purpose, were first sieved through a 45µm sieve. The polymer was dried in an air circulated oven at 120-140°C for 2 h prior to blending. Individual samples were prepared with 5, 10, 20, 30, 40 and 50 wt%, each of raw FAC and silane grafted FACs. A fully intermeshing co-rotating twin screw extruder (LabTech Engg. Co.Ltd. Thailand, Model No: LTE-20-40) was used for reactive extrusion with screw diameter 20 mm and 40:1 L/D ratio. Co-rotating screw extruder usually have uniform shear rate distribution in the segmented screw sections and attainment of distributive mixing of filler particles in the polymer matrix [28, 29]. The pre-dried polymer and FAC compound were extruded

through a circular die with diameter 50 mm with operating conditions at 280°C and rpm in the range of 20-25. Once the blends were extruded, the extrudates were water cooled, pulled and pelletized with the help of pelletizer. The pelletized granules of PC-FAC composite were pre dried at 90±5°C for 12 h and conditioning was done at 23-27°C for 24 h prior to characterization.

### 3. CHARACTERIZATION

#### 3.1 Thermal Decomposition Behaviour

Thermal analysis was executed for pristine PC, PC/ raw FAC and PC/ GFAC in a TGA/SDT A851° Mettler Toledo (USA). About 15 g of composite in a crucible was heated at a heating rate of 5°C/min from 25°C to 700°C in nitrogen flow of 50ml/min. The weight loss against temperature was measured, plotted and the char residue was observed.

#### 3.2 Morphological examination

FESEM studies of PC composites, untreated FAC and silane treated FAC were carried out on Carl Zeiss SIGMATM (Germany) FESEM. The samples were sputtered using Au-Pd for 75 seconds in 10 mA under the pressure of  $0.6 \times 10^{-2}$  Pa, tested in the microscope at 5kV and the images were obtained upto 20KX magnification.

#### 3.3 Compositional Analysis

PC, PC/ raw FAC and PC/ GFAC were analyzed using X-ray diffraction (XRD) on Bruker AXS D8 (U.S.A) Advanced Diffractometer with Cu K $\alpha$  radiation. Functional groups and fingerprints for chemical modification of FAC after silane grafting were analysed using FTIR spectroscopy. The spectrum was recorded between 4000 and 500 cm<sup>-1</sup> with KBr pellets at room temperature on Perkin Elmer Spectrum BS FTIR (U.S.) system.

## 4. RESULTS AND DISCUSSIONS

#### 4.1 Thermal Decomposition Analysis

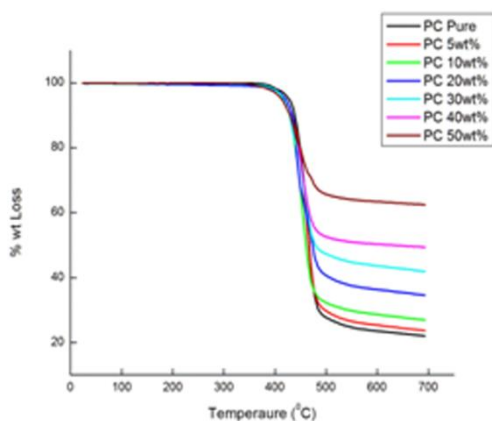


Fig. 2(a) - TGA thermograph of PC with raw FAC

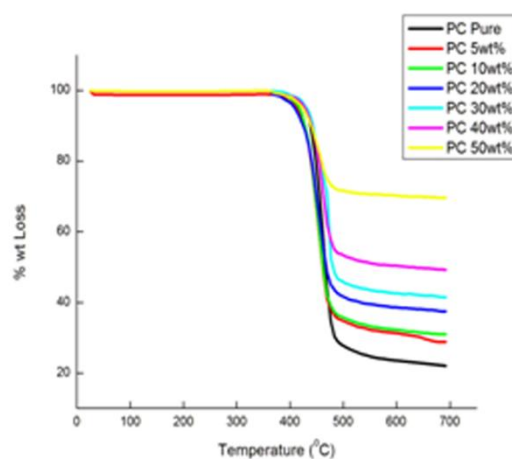


Fig.2(b) - TGA thermograph of PC with Silane grafted FAC

40

It was speculated that the flame retardancy of PC containing FAC caused by accelerating the thermal degradation rate of PC to ensure the formation of an insulating carbon layer on the surface that inhibited the supply of flammable gas and heat transfer [30,31]. When the thermal energy begins to surpass the bond energies of various bonds in the PC chains, a random chain scission takes place and the degradation rate increases rapidly. It is apparent that the lowest bond energies are 251 and 330 KJmol<sup>-1</sup> and these are assigned to the C-C bond of isopropylidene and the C-C bond of carbonate, respectively [32]. The influence of tiny amounts of individual additive on thermal degradation of PC was examined. Fig. 2(a) and 2(b) shows the decomposition thermographs of PC/ FAC composites with raw and grafted cenospheres. All the curves depict a single stage degradation pattern. The thermographs can be divided into three major zones: the first reaction zone (25 - 360 °C), where evolution of water, un-reacted oligomers and small groups such as methane, ethylene acetone were evaporated. In the second stage (350 - 480 °C), initial decomposition of various concentrations occurs at 350 °C, determining the onset of pyrolysis of the polymer. Over this zone, weight loss occurs due to thermal decomposition during pyrolysis. In the third zone (480 - 700 °C), as the concentration of FAC increases, increment in the thermal stability of composites is observed. The augmentation in thermal stability may be attributed to the restricted mobility of segmental movement of PC molecular chains which is due to the enhanced interaction between FAC and the polymeric matrix. Restriction of mobility of polymer chains by oxide particles present in FAC also contributes to the improvement observed in thermal stability [33]. The TGA graphs and Table 1 demonstrate an increase in residual char, with increase in FAC concentration. Char consists of carbonaceous porous turbostratic structure which assists in releasing the pyrolytic gases forming a negative flux against the convective flux of heat, thereby augmenting the thermal insulation.

75

Table 1 Char Residue

PC-UNTREATED FILLERS	CHAR RESIDUE	PC-TREATED FILLERS	CHAR RESIDUE
Pristine PC	22%	Pristine PC	22%
PC 5 WT%	23%	PC 5 WT%	28%
PC 10 WT%	27%	PC 10 WT%	31%
PC 20 WT%	34%	PC 20 WT%	38%
PC 30 WT%	41%	PC 30 WT%	43%
PC 40 WT%	50%	PC 40 WT%	55%
PC 50 WT%	62%	PC 50 WT%	70%

### Thermal Conductivity Models

The determination of thermal conductivity of PC/FAC composite is of paramount importance in thermal insulation applications of composite material. Maxwell identified the first theoretical model for thermal conductivity of two phase system by considering spherical fillers dispersed in a continuous matrix. He also assumed that these filler particulates had no thermal interaction with each other [34]. The spherical geometry of the cenosphere particles supports the Maxwell model for the calculation of thermal conductivity for present work. This model helps in establishing and validating the experimental results through mathematical modelling.

Here, two types of model are taken into consideration.

For parallel conduction model:

$$Kc = (1 - \varphi)Km + \varphi Kf \quad (4.1)$$

For series conduction model:

$$\frac{1}{Kc} = \frac{1-\varphi}{Km} + \frac{\varphi}{Kf} \quad (4.2)$$

The effective thermal conductivity of composite is given by geometric mean model:

$$Kc = Kf^\varphi \cdot Km^{(1-\varphi)} \quad (4.3)$$

Where k: thermal conductivity, c: composite, m: matrix, f: filler  
 $\varphi$ : volume fraction of filler

Maxwell depicted the exact solution for the conductivity of randomly distributed spheres in a homogeneous medium using the following equation [35].

$$Kc = Km \left[ \frac{Kf + 2Km - 2\varphi(Km - Kf)}{Kf + 2Km + \varphi(Km - Kf)} \right] \quad (4.4)$$

For present work

$K_m = 0.19 \text{ W/m}^\circ\text{C}$  (thermal conductivity of matrix i.e. PC)

$K_f = 0.11 \text{ W/m}^\circ\text{C}$  (thermal conductivity of filler i.e. FAC)

The above mathematical values were taken from the supplier data sheet.

Table 2 Thermal Conductivity Calculation

Calculated values of thermal conductivity ( $K_{eff}$ ) for all models					
Composition	Parallel (W/m- $^\circ\text{C}$ )	Series (W/m- $^\circ\text{C}$ )	Effective (W/m- $^\circ\text{C}$ )	Maxwell (W/m- $^\circ\text{C}$ )	Average
5wt% FAC	0.18	0.18	0.18	0.18	0.18
10wt% FAC	0.18	0.18	0.17	0.18	0.17
20wt% FAC	0.17	0.16	0.17	0.17	0.16
30wt% FAC	0.16	0.15	0.16	0.16	0.15
40wt% FAC	0.15	0.14	0.15	0.15	0.14
50wt% FAC	0.15	0.13	0.14	0.14	0.13

The thermal conductivity was computed for above four models and for each composition of PC/FAC composite using mathematical equations (4.1 to 4.4). Table 2 represents the average of calculated values of thermal conductivity for all compositions and for each model. From the above results, it can be inferred that the concentration of spherical cenosphere particles strongly influence the thermal conductivity value of pristine PC. With increment in the concentration of the FAC in the polymer matrix, significant decrease in the value of thermal conductivity for each model was observed. For further validation, TGA results were also commensurated with the mathematical results for thermal conductivity. Thermogravimetric analysis also shows the enhancement in the char residue with the increasing concentration of FAC, which reflects the formation of insulative layer on the polymer matrix. It acts as a thermal barrier and 29% decrement in the thermal conductivity value affirms the same. The percentage decrease in thermal conductivity is shown in Fig. 3 with the help of pie chart.

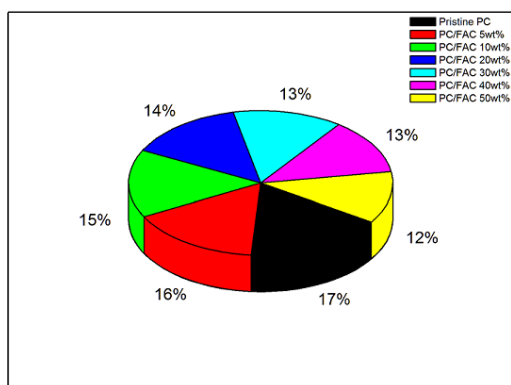


Fig. 3 - Pie chart for thermal conductivity values

#### 4.2 Compositional and Functional Group Analysis

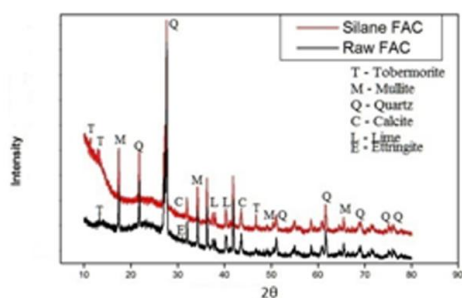


Fig 4(a) - XRD spectra of FAC

Fig 4(a) depicts the XRD spectra of raw FAC and silane grafted FAC. Five crystalline mineral phases were present in the FAC, namely tobermorite ( $\text{Ca}_5(\text{OH})_2\text{Si}_6\text{O}_{16}\cdot 5\text{H}_2\text{O}$ ), mullite ( $3\text{Al}_2\text{O}_3\cdot 2\text{SiO}_2$ ), quartz ( $\text{SiO}_2$ ), calcite ( $\text{CaCO}_3$ ), lime ( $\text{CaO}$ ) as shown in XRD spectra Fig. 4(a) [36]. It is evident that the major content of cenosphere is Quartz and Mullite, depicted as Q and M [37]. Mullite, being the most crystalline phase of FAC [38], was responsible for tremendous thermal stability, low thermal expansion, high creep resistance in highly oxidative and corrosive environments, high thermal shock resistance [14-19]. XRD spectra showed that the product was mostly mullite which reasserts the thermal stability of cenospheres. There was no evident change in raw FAC and Silane treated FAC in XRD spectra, except for one additional peak at  $2\theta$  value of  $11^\circ$ , which can be attributed to the silane coupling [39].

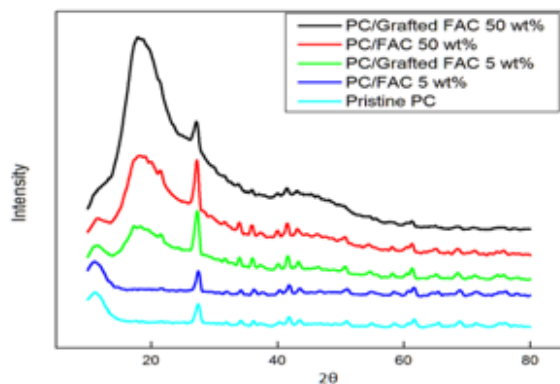


Fig 4(b) - XRD spectra for PC-FAC composite

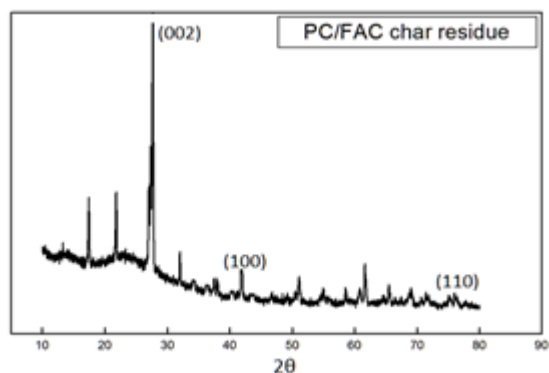


Fig 4(c)-XRD spectra for char

25

The XRD pattern of pure PC Fig. 4(b) shows three prominent peaks positioned at  $27.42^\circ$ ,  $41.65^\circ$ ,  $61.58^\circ$  which attributed to the interference along the axis of the main chain segment, interference between chains and short range correlations between phenyl groups on neighbouring chains respectively [40]. The FAC/ PC exhibited high similarity with raw and silane grafted FAC with respect to XRD pattern because the PC has a highly amorphous structure and has no sharp peaks of its own, therefore the crystalline phases of FAC are evident [41]. This proves that polymer matrix is inappreciably influenced by the concentration of cenosphere [42]. XRD pattern of decomposed composite is shown in Fig 4(c) which showed the peaks for turbostratic carbon and reflected the presence of some crystallinity in the char residue. The existence of the peaks corresponding to the (002), (100) and (110) reflections suggested that carbon in char has an intermediate structure called turbostratic between graphite and amorphous structure. The peak corresponding to the (100) reflection might be reflecting the merging of peaks, which hindered the amorphous nature of char and showed crystallinity [43].

Fourier Transform Infra red spectra shown in Fig 5(a) depict functional groups and fingerprint regions for FAC, and Silane grafted FAC. The spectrum showed Si-O-Si asymmetric stretching vibration centered at  $1081\text{ cm}^{-1}$ , representing the presence of internal  $\text{SiO}_4$  tetrahedra structure in both raw and silane treated FAC [44]. A peak related to (Si-O) bond stretching vibration of compound  $\text{Si}(\text{OC}_2\text{H}_5)_4$  appeared around  $787\text{ cm}^{-1}$  in silane treated FAC [45]. Additional peaks were evident in Silane Grafted FAC at  $2363\text{ cm}^{-1}$  which could be assigned to C-H stretching vibration of organic functional group due to silane coupling agent. An additional peak  $2930\text{ cm}^{-1}$ , corresponding to the flexible vibration of hydroxyl group (OH) group indicated the interaction between silane and FAC, hence establishing and confirming effective coupling [46].

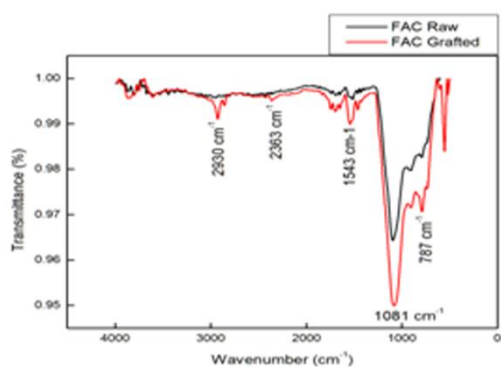


Fig 5(a) - FTIR spectra for FAC and grafted FAC

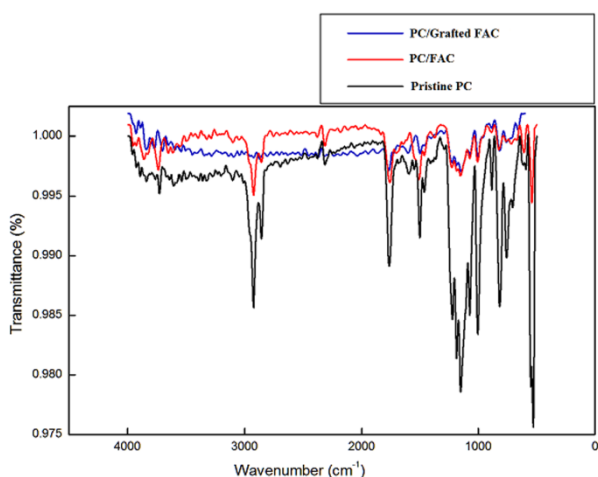


Fig 5(b) - FTIR spectra for PC composites

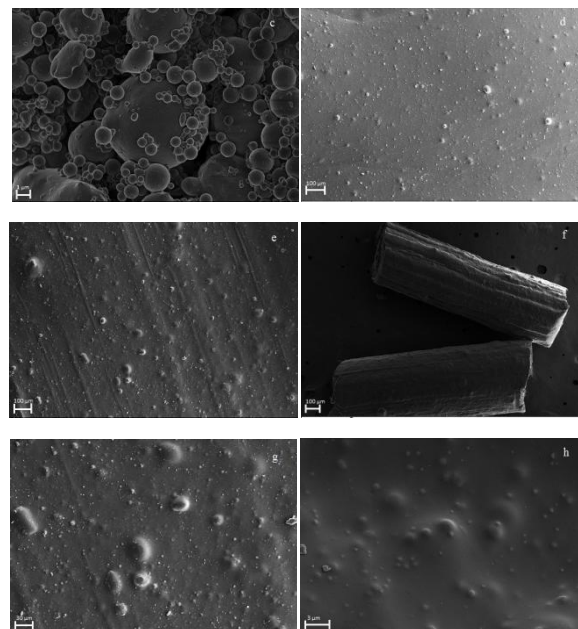


Fig 6 - FESEM images of FAC and PC-FAC composite

Fig 5(b) shows signature peaks for Polycarbonate depicting the appearance of an intense triplet 1,154, 1,194 and 1,219  $\text{cm}^{-1}$ . Despite the presence of a carbonyl group, at 1,774  $\text{cm}^{-1}$ , the strongest infrared absorptions in polycarbonate were due to the C-O single bond stretches. Additional C-O related peaks continue down to 1,000  $\text{cm}^{-1}$ , with the strongest of these at 1,016  $\text{cm}^{-1}$ . Among the aromatic ring breathing modes, only the 1,506  $\text{cm}^{-1}$  peak was relatively intense. While the methyl stretch at 2,970  $\text{cm}^{-1}$  was weak, it was noticeable due to the absence of other peaks in this region [46]. FTIR spectra for PC-FAC composite showed the characteristic peaks of both PC and silane grafted FAC which inferred that there was uniform distribution of silane grafted FAC in the PC matrix.

### 4.3 Morphological Examination

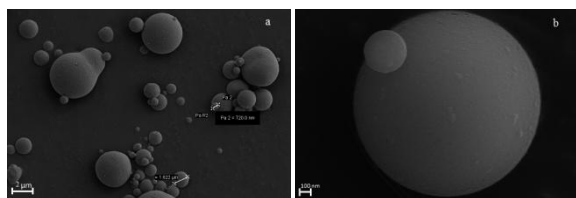


Fig. 6 shows FESEM images of raw FAC Fig 6(a)(b) Silane treated FAC Fig 6(c), 5 wt% PC/ FAC Fig 6(d), 5 wt%PC/ Grafted FAC Fig 6(e), 50 wt% pellets Fig 6(f), 50 wt% PC/FAC Fig 6(g) and 50 wt%PC/ Grafted FAC Fig 6(h). Figures 6(a)(b) and (c) clearly show change in morphology of cenospheres. Raw untreated cenospheres had smooth and globular morphology while the grafted FAC particles possessed a comparatively rougher surface. Small and numerous granular particles were seen attached to the surface of the treated FAC [21], confirming surface modification and aiding molecular lever adhesion between PC and FAC. As depicted clearly in Fig 6(d), the cenospheres were loosely dispersed in the PC matrix, most of the particles seemed to be weakly attached on the surface. Alternatively, in Fig 6(e), a tight embedded and mechanically interlocked morphology of the cenosphere in the resin matrix was evident, upon incorporation of treated FACs. Extruded composite in the form of pellet is clearly shown in the Fig 6(f) which demonstrated the retention of spherical nature of the cenosphere particles. Figures 6(g)(h) represents the morphology of 50 wt% PC/FAC composite with more number of cenosphere particles and uniform distribution which indicated good state of dispersion of the particles and a fewer number of unbound cenospheres [41].

### Conclusion

In this study, a novel approach towards research has been established by the generation of PC-FAC composite and characterized through FESEM, TGA, FTIR and XRD. The effectiveness of the PC-FAC composite was examined on the basis of thermal analysis and thermal conductivity was computed mathematically. Effective coupling of FAC and silane agent was established and confirmed by FTIR spectra. Thermogravimetric analysis reflected tremendous increment in the char residue from 22% to 70% with the increase in the concentration of filler which reasserted the insulation behaviour of the cenosphere particles. Each TGA thermograph was the average of five samples analysed

by TGA which decreases the chances of error in the experimental results. The mathematical calculation inferred 29% decrement in the value of thermal conductivity of the composite. This novel approach opens the door for further research in the field of thermoplastic polymer. By tailoring the properties and incorporation of fillers in thermoplastic polymers, the applications can be extended in the fields of insulative coatings for automotive industry, Car battery casings, aircraft canopy, locomotive windshield laminates and military transparent armour.

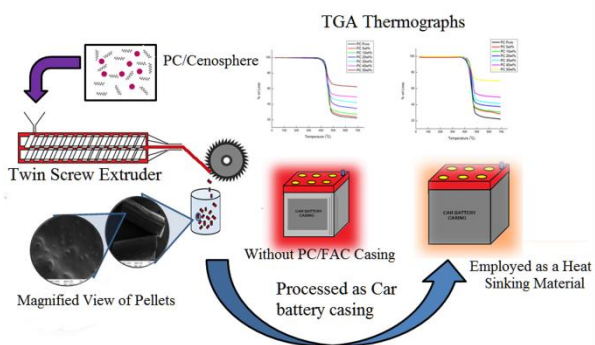
## Acknowledgements

The authors appreciate Defence Institute of Advanced Technology for financial support. Also, we would like to thank Dr. Prahlada, Vice Chancellor, DIAT-DU for continuous encouragement and support and DIAT-DRDO Nano Project Program (EPIPR/1003883/M/01/908/2012/D (R&D/1416 Dated: 28.03.2012, DRDO HQ, New Delhi for financial assistance. The authors would also like to acknowledge Mr. H.H.Kumar and his group members, Armament Research and Development Establishment Pune, for providing continuous support. We are also grateful to Dr. P. Alegaonkar, Dr. A. Abhyankar, Dhananjay Gunjal for continuous technical support and also thankful to Prajith P., Yutika Badhe and Rajat Arora for their technical support.

## References

- [1]. A. Arizmendi-Morquecho, A. Chávez-Valdez, J. Alvarez-Quintana. *Appl. Therm. Eng.* 2012, 48, 117.
- [2]. A. Chávez-Valdez, A. Arizmendi-Morquecho, G. Vargas, J.M. Almanza, J. Alvarez-Quintana. *Acta Mater.* 2011, 59 (6), 2556.
- [3]. M.V. Deepthi, Madan Sharma, R.R.N. Sailaja, P. Anantha, P. Sampathkumaran, S. Seetharamu. *Mater. Des.* 2010, 31(4), 2051.
- [4]. Elena V. Fomenko, Natalia N. Ashits, Marina V. Pankova, Leonid A. Solovyov, Alexander G. Anshits.: 'Fly Ash cenospheres: Composition, Morphology, Structure and Helium Permeability in World of Coal Ash Conference. Denver, CO, USA', (2011).
- [5]. Khairul Nizar Ismail, Kamarudin Hussin, Mohd Sobri Idris. *Journal of Nuclear and Related Technologies.* 2007, 4, 47.
- [6]. Raask E. *Journal of the Institute of Fuel.* 1968, 43(332) , 339.
- [7]. Raask E. *Journal of the Institute and Fuel.* 1969, 48 , 366.
- [8]. Elena V. Fomenko, Natalia N. Anshits, Leonid A. Solovyov, Olga A. Mikhaylova, Alexander G. Anshits. *Energy fuels.* 2013, 27, 5440.
- [9]. Bibby, D. M. *Fuel.* 1977, 56 , 427
- [10]. Stanislav V. Vassilev, Christina G. Vassileva. *Fuel Process. Technol.* 1993, 47(3) , 261.
- [11]. Ling-ngee Ngu, Hongwei Wu and Dong-ke Zhang. *Energy Fuels.* 2007, 21 (6) , 3437.
- [12]. P. K Kolay, D. N. Singh. *Cem. Concr. Res.* 2001, 31 , 539
- [13]. S.V. Vassilev, R.Menendez, M.Diaz-Somoano, M.R. Martinez- Tarazona. *Fuel.* 2004, 83, 585.
- [14]. S. Varadarajan , AK Patanaik , VK Sarin. *Surf. Coat. Technol.* 2001, 139, 153.
- [15]. Cao X., Vassen R, Stoeber D. *J. Eur. Ceram. Soc.* 2004, 24(1) , 1.
- [16]. Bartuli C., Lusvarghi L., Manfredini T., Valente T. *J. Eur. Ceram. Soc.* 2007, 27(2-3) , 1615.
- [17]. Ramaswamy P., Seetharamu S., Varma K.B., Rao K.J. *J. Therm. Spray Technol.* 1998, 7(4) , 497.
- [18]. Rohan P., Neufuss K., Matejcek J., Dubsky J., Prchlik L., Holzgartner C. *Ceram. Int.* 2004, 30 , 597.
- [19]. Schneider H., Schreurer J., Hildmann B. *J. Eur. Ceram. Soc.* 2008, 28, 329.
- [20]. Esteban I, Santiago P., José M., Cano J., Galante M, Pettarin V, Bernal C. *Mater Des.* 2014, 55 , 85.
- [21]. Wang C, Wang D, Zheng S. *Mater. Lett.* 2013, 111 , 208.
- [22]. Chauhan S.R., Thakur S. *Mater Des.* 2013, 51, 398.
- [23]. Jiang W, Tjong S. *Polym. Degrad. Stab.* 1999, 66 , 241.
- [24]. Bassam A. Sweileh, Yusuf M. Al-Hiari, Mohammad H. Kailani, Hani A. Mohammad. *Molecules.* 2010, 15 , 366.
- [25]. Tingju L, Man J, Zhongguo J, David H, Zeyong W., Zuowan Z. *Composites Part B.* 2013, 51 , 28.
- [26]. Hye-Jung Kang, Wiriya Meesiri, Frank D. Blum. *Mater. Sci. Eng., A.* 1990, 126(1-2) , 265.
- [27]. Edwin P. Plueddemann. *Silane Coupling Agents.* Springer, (1982) .
- [28]. B.D.Favis, D Therrien. *Polymer.* 1991, 32(8) , 1474.
- [29]. Frank Goffreda, Allan Griff, Larry Livinghouse, Tom Walsh, Joseph Scuralli.: *Tool and Manufacturing Engineers Handbook Knowledge Base.* Society of Manufacturing Engineers (1998).
- [30]. Yuezhan Feng, Bo Wang, Fangfang Wang, Yuanxu Zhao, Chuntai Liu, Jingbo Chen, Changyu Shen. *Polym. Degrad. Stab.* 2014, 107, 129.
- [31]. Alberto Ballistreri, Giorgio Montaudo, Emilio Scamporrino, Concetto Puglisi, Daniele Vitalini , S. Cucinella. *J. Polym. Sci. A Polym. Chem.* 1988, 26(8) , 2113.
- [32]. J.L.Koenig. *Spectroscopy of polymers .* Elsevier (1999)
- [33]. Sanjib Baglari, Madhusree Kole, T K Dey. *Indian J. Phys.* 2011, 85(4) , 559.
- [34]. Maxwell James Clark. *Electricity and Magnetism.* Oxford, Clarendon press (1873).
- [35]. Serhat DURMAZ. :A numerical study on the effective thermal conductivity of composite material. PhD thesis, Graduate School of Natural and Applied Sciences of Dokuz Eylul University, January (2004).
- [36]. Sammy M. Nyale, Omotola O. Babajide, Grant D. Birch, Nuran Böke, Leslie F. Petrik. *Procedia Environmental Sciences.* 2013, 18 , 722.
- [37]. Wei Wang, Qin Li, Bing Wang, Xiao-Tian Xu, Jian-Ping Zhai. *Mater. Chem. Phys.* 2013, 135(2-3) , 1077.
- [38]. Colin R. Ward , David French. *Fuel.* 2006, 85(16) , 2268.
- [39]. Navin Chand, Prabhat Sharma, M. Fahim. *Mater. Sci. Eng., A.* 2010, 527(21-22) , 5873.
- [40]. Ryan T. Chancey, Paul Stutzman , Maria C.G. Juenger , David W. Fowler. *Cem. Concr. Res.* 2010, 40 , 146.
- [41]. T Matsunaga, J.K Kim, S Hardcastle, P.K Rohatgi. *Mater. Sci. Eng., A.* 2002, 325(1-2) , 333.
- [42]. Arijit Das, Bhabani K. Satapathy. *Mater Des.* 2011, 32 , 1477.
- [43]. Z.Q. Li, C.J. Lu, Z.P. Xia, Y. Zhou, Z. Luo. *Carbon.* 2007, 45(8) , 1686.
- [44]. Stuti Katara, Sakshi Kabra, Anita Sharma, Renu Hada, Ashu Rani. *International Research Journal of Pure & Applied Chemistry.* 2013, 3(4) , 299.
- [45]. R. G. Kraus, E. D. Emmons, J. S. Thompson, A. M. Covington. *J. Polym. Sci. B Polym. Phys.* 2008, 46(7) , 734.
- [46]. Xianbo Huang, Xiaoyue Ouyang, Fanglin Ning, Jianqi Wang. *Polym. Degrad. Stab.* 2006, 91(3) , 606.

## Graphical Abstract



25

30

5

35

## Figure Caption

10 **Fig.1-** Schematic representation of Silane Grafting of cenosphere.

**Fig.2 -** (a) TGA thermograph of (a) PC with raw FAC (b) PC with silane grafted FAC.

40

**Fig.3-** Pie chart for thermal conductivity values.

**Fig.4-** XRD spectra of (a) FAC (b) PC-FAC composite (c) char residue.

**Fig.5-** FTIR spectra for (a) FAC and grafted FAC (b) PC/FAC Composite.

**Fig.6-** FESEM image of (a) raw FAC (b) raw FAC at 15.00kV (c) silane grafted FAC (d) 5 wt% PC/ FAC (e) 5 wt% PC/ Grafted FAC (f) 50 wt% PC/FAC pellets (g) 50 wt% PC/ FAC (h) 50 wt% PC/ Grafted FAC

45

50

55